Progress In Electromagnetics Research C, Vol. 65, 191–200, 2016

Generation, Application and Analysis of a Novel Family of m-segment Quadratic Fractal Curves to Antennas

Rajas P. Khokle*

Abstract—A novel family of fractal curves is proposed which provides the designer a systematic way of miniaturizing the microwave components with the freedom of choosing among form factor, design complexity and achieved miniaturization. The proposed fractal curve is characterized by two integer values m and n. The m value determines the form factor of the fractal while n value governs the iteration number. The equations governing the geometry of fractals are also presented. The proposed fractal is characterized for miniaturization by designing a printed monopole antenna for various values of m and n. The results from the full wave simulations and experiments are analysed and explained. The effect of fractal on reducing the resonant frequency is quantified by an equation based on its physical interpretation. Based on this analysis, saturation point for miniaturization is established. The curves being symmetric around a straight line, distortionless radiation patterns are seen.

1. INTRODUCTION

In this paper, a new family of fractal curves which can be used to miniaturize the microwave components is introduced. The electromagnetic properties of fractals are thoroughly discussed in [1–3], and it is well established that they are able to miniaturize microwave components. When used for antennas, they provide frequency compression, multi-resonant behaviour, and the design approaches small antenna limit. When they are applied to filters, along with size reduction, they provide harmonic suppression, and wideband or multiband operation [4, 5]. A lot of techniques exist in literature for miniaturization of microwave components such as dielecric loading, magnetic loading, use of lumped components, metamaterial loading and use of optimization algorithms [6]. Using fractals is one important tool in the hand of microwave engineer. Fractals are the mathematical descriptions of fractured geometries which incorporate twists and bends according to some predefined rules and operations. One of the important properties of such curves is to have an infinite length curled up in a finite volume. This phenomenon is time and again exploited by the antenna and microwave community for miniaturization. While arbitrary bending and twisting may produce better compression in some cases, it is largely an optimization problem to be solved using simulation software, rather than a systematic approach that can be employed by the common antenna designer.

In [7], one can find an excellent description and analysis of fractals for miniaturizing dipoles, increasing the input impedance of loops, compacting linear phased arrays and widening their scanning ability. The authors of [8] also described the theory and design of an antenna array utilizing the fractal geometry. Fractals are deployed in patch antennas of various shapes [9, 10]. They are also utilized in slot and helix type of antennas [11, 12] for multiband, multimode operations. They are also employed in combination as in [13], where authors have combined Sierpinski and Koch fractal curves to create a dipole antenna. In [14], the Koch fractal is utilized to design a circularly polarized UHF RFID antenna. In [15], a dielectric loaded fractal design is proposed for heptaband operation. Recently, fractals are also being utilized to create the textile antennas [16], where they are subjected to bending and wetting

Received 20 April 2016, Accepted 30 June 2016, Scheduled 8 July 2016
* Corresponding author: Rajas Prakash Khokle (Rajas-prakash.khokle@students.mq.edu.au).
The author is with the Department of Engineering, Macquarie University, Australia.

and their characteristics in presence of human body are analysed. While the traditional fractals like Koch, Sierpenski, Minkowksi and Hilbert were being investigated for their electromagnetic properties, some researchers randomized the geometry parameters of these fractal curves (like angles, lengths and line thickness) and then used the optimization algorithms like Particle Swarm optimization (PSO) and Genetic Algorithm (GA) to obtain the acceptable performance in various frequency bands like GPS and WiMax [17–19]. Recently, this approach is also utilized to design diplexers with superconducting antennas that find application in radio astronomy [20]. Not only at microwave frequencies, but they are also employed at terahertz range for miniaturizing split ring resonator [21] which is the most extensively studied structure for metamaterials. The localization of electromagnetic waves in 3D photonic fractals is also demonstrated and explained in [22, 23]. It is also employed to enhance bandwidth in Left handed Metamaterials [24]. These are just a few examples to demonstrate that the fractals are still employed to design different microwave components to achieve better or novel electromagnetic properties for diverse applications.

In most of the fractal geometries reported till date, it is the iteration number alone that decides the resonant frequency. Consequently, with the given initial length, the resonant frequencies and the form factors (length to width ratio) are fixed. Thus, the designer does not have any freedom or trade-off with form factor and frequency response of the device. In this paper, a way to generate a family of fractal curves is presented which gives this freedom to the designer. To the best knowledge of the author, no such fractal is available in the open literature. So the aim of the present work is to introduce such a fractal geometrical construct and to equip the designer with the knowledge of trade off among the miniaturization achieved, form-factor and fabrication complexity of the design.

Following this introduction, the modus operandi to generate the new fractal geometry and the characteristic equations that describe the various parameters of the proposed curve are presented. It is followed by its application to the monopole antenna to characterize the resonance properties. The proposed construct is then compared with the standard Von Koch curve to understand and quantify its electromagnetic properties. The advantages of proposed fractal are also established. Then the results are discussed from the point of view of miniaturization and the expressions are developed to predict maximum miniaturization possible and the resonant frequency achieved with various iterations. The proposed fractals are also analysed by computing their lacunarity dimensions [25, 26]. This gives comprehensive information about the proposed fractal geometry. Finally, the conclusion is made.

2. GENERATION AND CHARACTERIZATION OF FRACTALS

Figure 1 shows the geometry and the process of generation of different iterations of the proposed fractal curve. This fractal is generated and characterized by using 2 integer values $m \geq 2$ and $n \geq 0$ where m is (seed) value corresponding to the number of segments a straight line (0th iteration) of length 'L' will be divided whereas n corresponds to the iteration number. It can be noted that $n = 0$ always corresponds to a straight line irrespective of the value of m. The fractal can be generated by the use of 2 labels 'A' and 'B' and 2 operations 'p' and 'q'. The operations 'p' and 'q' are defined as follows:

$p \rightarrow$ Turn 45° clockwise, go forward till distance $L/(m\sqrt{2})$, then turn anticlockwise by 90°, go forward by distance $L/(m\sqrt{2})$.

$q \rightarrow$ Turn 45° anticlockwise, go forward till distance $L/(m\sqrt{2})$, then turn clockwise by 90°, go forward by distance $L/(m\sqrt{2})$.

If operation 'p' ('q') is performed on a line segment, then every new line generated should be labelled 'A' ('B') respectively. Next iteration will be generated based upon this label. The straight line of 0th iteration can be labelled 'A' or 'B' arbitrarily. It can be noted that each of these operations generates two line segments forming a right angle and hence the name quadratic fractal. In order to have a symmetry, the processes of generating fractal for even and odd values of m are slightly different. If m is an odd integer, then for a line segment having label 'A', the sequence of performing operations to obtain next iteration is $A \rightarrow (pqp\ldots)_m$ while for a line segment having label 'B' the sequence of operations is $B \rightarrow (qpq\ldots)_m$. If m is an even integer, irrespective of label, the operations have to be performed alternately, i.e., A or $B \rightarrow (pqpq\ldots)_m$. In both the cases, the subscript m denotes the number of times of operations to be performed. For example for $m = 4$, the sequence of operation would be $A \rightarrow$ '$pqpq$' while for $m = 5$, it would be $A \rightarrow$ '$pqpqp$'. This process of generating 1st and 2nd

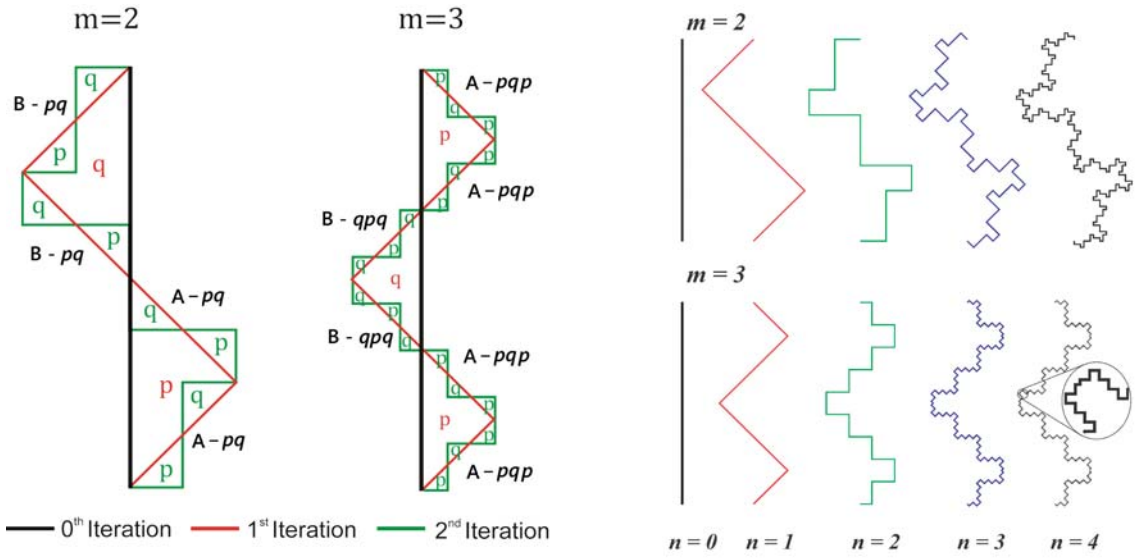

Figure 1. (a) Generating fractal iterations for even and odd value of m, using the operations 'p' and 'q'. (b) First 4 fractal iteration stages for $m = 2$ and $m = 3$ family.

iteration from 0th iteration (straight line) is shown in Fig. 1(a) for $m = 2$ and $m = 3$. The first five iterations from $n = 0$ to $n = 4$ for $m = 2$ and $m = 3$ are shown in Fig. 1(b). It can be pointed out that it is not necessary to use the same seed value m for generating successive iterations. For example, as shown in Fig. 2(Line), $m = 2$, $m = 3$ and $m = 4$ are used to generate first,second and third iteration respectively. Thus, with the different permutations and combinations of m and n, one can get different linear geometries with the different form factors. The fractal can also be used to generate closed loops. Fig. 2 shows a loop generated by using $m = 3$, $n = 3$ fractal on the sides of a hexagon. Such closed structures can also be filled to create the patch resonators. In Fig. 2, the patch shows a outer square patch whose sides are modified by the $m = 3$, $n = 3$ curve. Inside this patch, another square modified by $m = 2$, $n = 3$ fractal is cut out as a slot. Inside this slot, a square patch which can be treated as scaled 0th iteration, is introduced. These examples are provided to show the versatility of the proposed m-Segment Quadratic fractal curve. It is the imagination of designers that would limit the conception of novel and convoluted geometries possible with this fractal.

$$\text{Number of parts} = (2m)^n \tag{1}$$

$$\text{Length of each part} = L/(m\sqrt{2})^n \tag{2}$$

$$\therefore \text{ Housdorff Dimension} = D = \frac{\log(2m)}{\log(m\sqrt{2})} \tag{3}$$

$$\text{Total Length of curve} = L(\sqrt{2}^n) \tag{4}$$

Eqs. (1) to (4) characterize the proposed fractal geometry. Eqs. (1) and (2) give the number and size of line segments that would be generated for a given value of m and n from a single straight line. It can be seen that the number of line segments grows with the nth power of $2m$ while the length of each part reduces with the nth power of $m\sqrt{2}$. Consequently, the Housdorff dimension (Eq. (3)) changes with the value of m and hence the proposed structure is termed as a family of m segment fractal curves. Eq. (4) clearly shows that the total length of curve is independent of the seed value m. So, theoretically the resonance should occur at same wavelength irrespective of m value. However, it is a well known fact that the perturbations smaller than the wavelength have lesser effect on an electromagnetic wave. As seen from (2), higher the value of m, smaller is the length of segments. So even for the same iteration across various values of m, the effectiveness of fractal curve would be different and so the structure is expected to resonate at different frequency. This is a remarkable property of the proposed

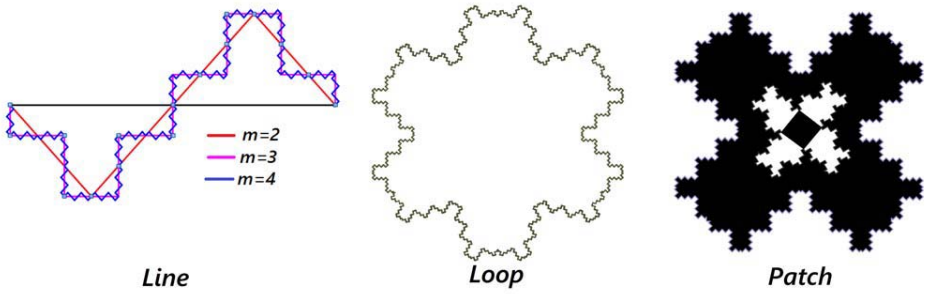

Figure 2. Example of different types of geometries possible with proposed fractal construct.

construct. One can start with the same length and can get many different resonant values with the combinations of m and n. A close inspection of the width of the proposed curve reveals that the width changes only with the odd number of iteration. The half width of the even iteration is same as that of its previous odd valued iteration. Since the structure is symmetrical in terms of width around the central axis (0th iteration line), calculating width for half of the structure (distance from tip to the center) suffices. The half width of the structure for odd value of n can be calculated by a series sum $\frac{L}{(2m)} + \frac{L}{(2m)^3} + \frac{L}{(2m)^5} + \ldots + \frac{L}{(2m)^n}$. Using this expression, one can calculate the required form factor by doubling the half width. Usually, for all practical applications in microwaves, considering the first two terms above series should be enough.

3. ANTENNA DESIGN AND FABRICATION

In order to evaluate the electromagnetic properties of the proposed fractal family, antennas with the values of $m = 2$ to 5 and $n = 1$ to 4 are designed and compared with the straight line monopole ($n = 0$). To generate the fractals for different values of m and n, a MATLAB program is written according to the modus operandi described above. The co-ordinates of the fractal so generated, are exported to HFSS to design a printed monopole antenna to perform full wave analysis. The fractal monopoles are designed on a metallic ground plane fed coaxially using an SMA connector. All the antennas are fabricated on commercially available FR4 substrate with $\epsilon_r = 4.7$, $\tan\delta = 0.02$ and height 1.6 mm. At this point, it

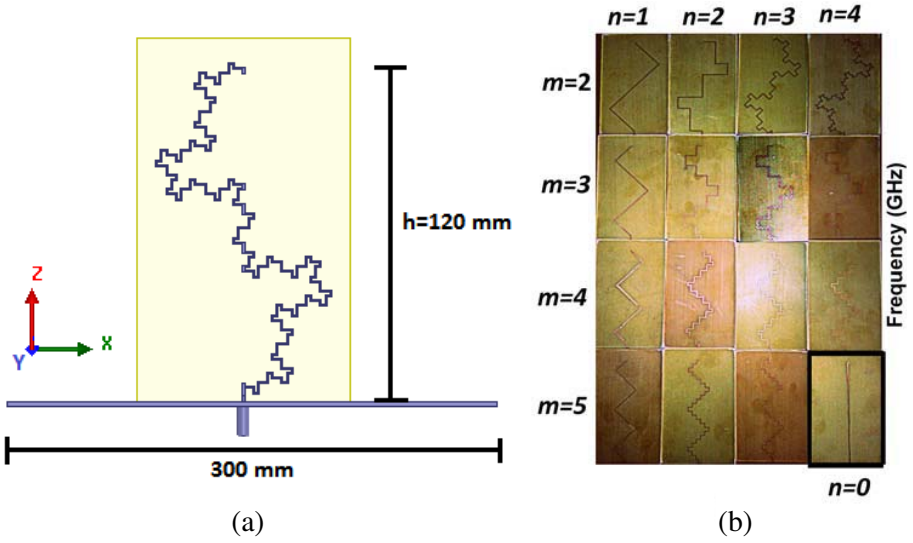

Figure 3. (a) Orientation of ($m = 2$, $n = 4$) antenna in co-ordinate system. (b) Photograph of the fabricated fractal antennas.

is useful to evaluate the complexity of the fractals and effect of m and n from the fabrication point of view. For this purpose, we compare two antennas, viz. $m = 4$, $n = 4$ and $m = 5$, $n = 3$. Using (1), the total number of parts are 4096 and 1000 respectively. From (2) the length of each part can be calculated as $L/1024$ and $L/353.55$. Thus, it can be seen that the antenna $m = 5$, $n = 3$ is easier to fabricate as the smallest length of part is more than that of $m = 4$, $n = 4$ antenna. Also, as the number of parts is smaller, so the time required for fabrication using standard milling machine setup is less for $m = 5$, $n = 3$ antenna. It can be noted that this parameter may not be an issue for photo etching fabrication process, as all the antennas will take same time. The antenna with $m = 5$ and $n = 4$ has the required line width of 15 µm with total number of parts $= 10^4$, each having length 48 µm. The available milling machine setup has the limitation of 100 µm dimension. So, $m = 5$ and $n = 4$ antenna is too complex and cannot be fabricated. The orientation of one of the antennas ($m = 2$, $n = 4$) in co-ordinate system is shown in Fig. 3(a). A photograph of all the fabricated antennas is shown in Fig. 3(b).

4. RESULTS AND ANALYSIS

The fabricated antennas are tested using Agilent N5222A Vector Network Analyser. The analysis of the proposed fractal is done by comparing the results of the proposed fractal with standard Von Koch fractal reported in [1]. First, the measured results are discussed from their input impedance point of view. It is followed by the analysis of their resonant frequencies. An expression for determining resonant frequency from the geometry parameters m and n is developed. Finally, the proposed fractals are analysed in terms of their lacunarity dimension.

The measured input impedance of the antennas is plotted in Fig. 4. The figure is split into four graphs, each showing the comparison of members from a single family of the proposed curve. It can be seen that the 0th iteration is same across all the families, from $m = 2$ to $m = 5$. This is obvious as it corresponds to a straight Euclidean line. The measurement of this 0th iteration is used as reference in all the graphs. From the results, it can be noticed that the resonant frequency decreases with increasing iteration number. Also, the real part of impedance increases with increasing iteration number. To further explore, analyse and quantify the proposed family of fractal curves, a comparison with the standard Koch curve is made. First five iterations ($n = 0$ to $n = 4$) of the Koch curve as reported

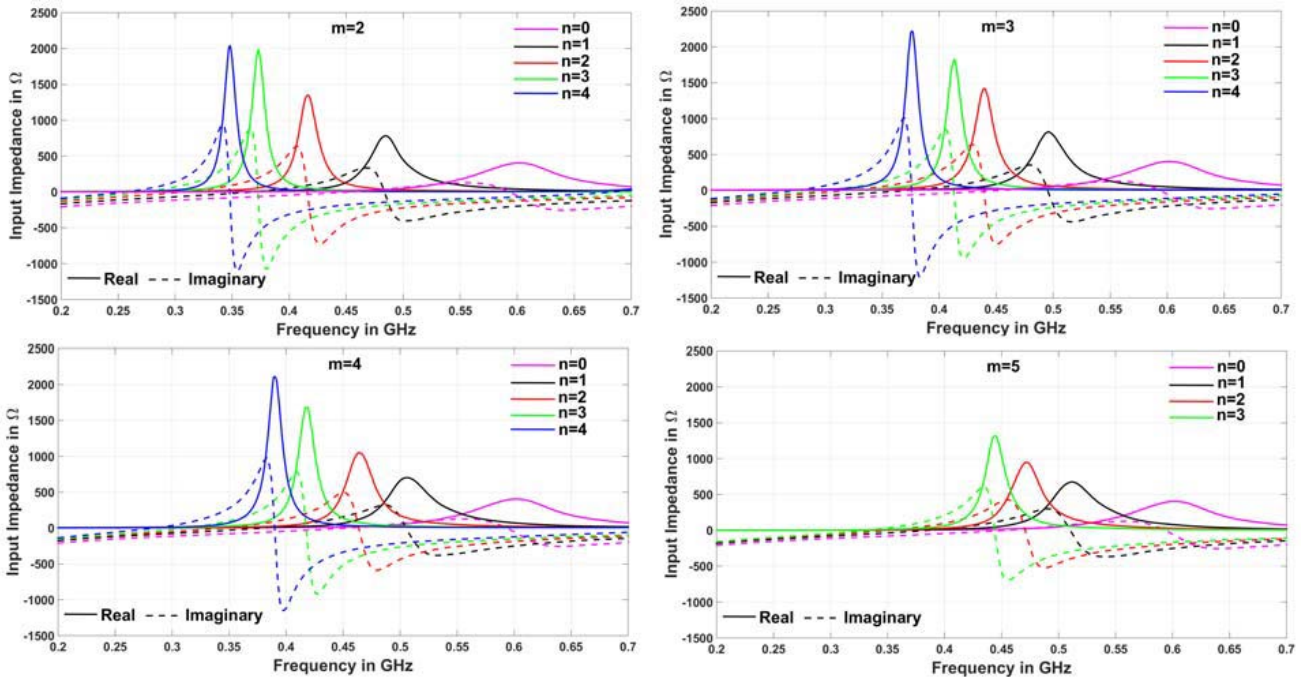

Figure 4. Measured input impedance of the fabricated fractal antennas.

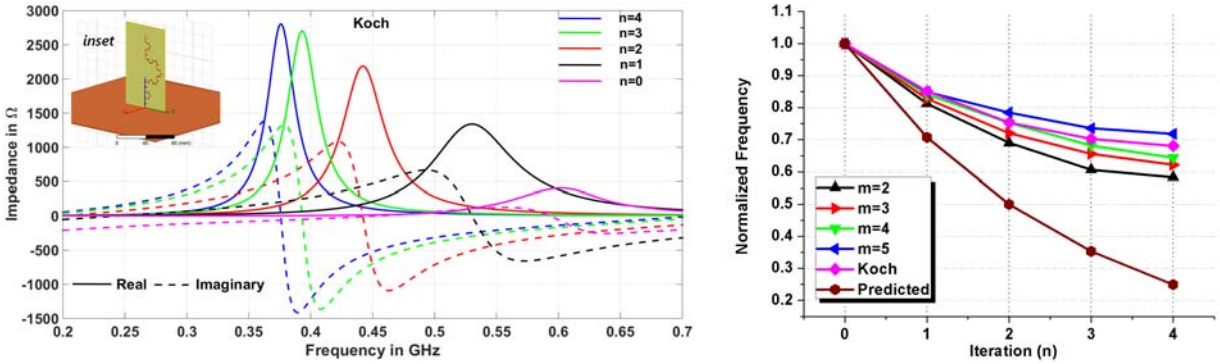

Figure 5. (a) Simulated input impedance of the first five iterations of the Koch fractal curve (inset: Orientation of Koch fractal antenna in HFSS. (b) Comparison of the measured normalized resonances for the different iterations of antennas ($n = 0$ to $n = 4$) of different families ($m = 2$ to $m = 5$) of proposed curve, with iterations of Koch fractal curve.

in [1] are generated using MATLAB and exported to HFSS for full wave simulation. The starting length of the Euclidean line is taken same as that in our proposed curve (120 mm). The simulated input impedances of the various iterations of the Koch curve are plotted in Fig. 5(a). The similarity in the nature of the graphs of Fig. 4 and Fig. 5, shows that the proposed m-segment quadratic fractal shows the characteristic behaviour of the fractal geometry.

For the quantitative analysis, the resonances of all the antennas are normalized with respect to the resonant frequency of the 0th iteration. Fig. 5(b) shows the comparison of the measured normalized resonances for the different iterations of antennas ($n = 0$ to $n = 4$) of different families ($m = 2$ to $m = 5$) of proposed curve along with the Koch fractal. It can be seen that the families $m = 2$, $m = 3$ and $m = 4$ are better than Koch curve in terms of miniaturization. The response of Koch curve is in between that of $m = 4$ and $m = 5$ family. For the Koch curve, the total width can be calculated as 34.6 mm. For $m = 4$ family, the total width is nearly 30 mm while it is 24 mm for $m = 5$ family. Taking the average of two widths, there is a reduction of almost 22% in terms of width, by the use of proposed curve. Thus, we can conclude that for similar resonance response, the proposed fractal saves about 22% of space than Koch curve.

Next, it can be noted that as the value of m increases, the rate of decrease in resonant frequency with iteration number is reduced. Thus, even though the same iteration (i.e., same value of n) from different families of curves has same geometrical length, their resonant frequencies are different. As m increases, the resonant frequency for the same value of n also increases. This behaviour proves that the smaller length of segments have smaller effect on miniaturization, irrespective of total geometrical length. Also, in Fig. 5(b), the resonance predicted by equating geometrical length to electrical length ($\lambda_{eff}/4$)) for the proposed geometry is plotted. It also shows that although the use of fractal geometry increases the geometrical length of the curve, it does not increase the electrical length of corresponding antenna at the same rate. From this plot of normalized resonances, it can be seen that electromagnetic miniaturizing ability of the fractal decreases with increasing fractal iteration. Such an exponential behaviour of the resonant frequencies can be captured by fitting the normalized experimental data in equation of the form

$$\frac{f_n}{f_0} = ae^{-bn} + c \tag{5}$$

where f_0 is the resonant frequency of the 0th iteration, and n is the same as the iteration number. a and b are the coefficients of curve fitting. Now as n goes to ∞, we get the lowest possible resonant frequency or saturation frequency, i.e., 'c' in above equation represents the saturation frequency and indicates maximum miniaturization possible for a given mth member of the fractal family. For $n = 0$, $f_n/f_0 = 1$, which implies $c = 1 - a$. With this understanding, the curve fitting is done using MATLAB.

The corresponding expressions are given by Eq. (6). The fitness of the curve is usually evaluated using degree of freedom adjusted R^2. It is the ratio of sum of square of regression and total sum of squares adjusted for degree of freedom. This parameter measures the correlation between the response values and predicted response values. The minimum adjusted R^2 for the proposed curve fit is 0.9983. It means that the equation explains the 99.83% of the data. The maximum RMS error is 0.0078 for $m = 2$ with maximum error of 0.01 at $m = 2$, $n = 3$. Thus the curve fit is excellent, and the expressions closely represent the resonant frequencies of the antennas.

$$\frac{f_n}{f_0} = \begin{cases} 0.5289e^{-0.4681n} + 0.4711, & m = 2 \\ 0.4854e^{-0.4519n} + 0.5146, & m = 3 \\ 0.3998e^{-0.5135n} + 0.6002, & m = 4 \\ 0.3194e^{-0.6207n} + 0.6806, & m = 5 \end{cases} \tag{6}$$

These equations can be further condensed and generalized by expressing the coefficients in terms of m as given in Eq. (7). Substituting Eqs. (7) into Eq. (6), one can predict the resonant frequency for any value of m and n. It should also be noted that the equation is valid for $m \geq 2$. Also as $m = (0, 1)$ would mean dividing a line in 0 or 1 parts, it does not make sense to input $m = 0$ or 1 in the proposed expression.

$$a = -0.06841m + 0.6653; \quad b = 0.04854m + 0.3522; \quad c = 0.06841m + 0.3347 \tag{7}$$

Further, the average lacunarity dimension for all fractal antennas Λ_{avg} is calculated by the methodology proposed in [25]. The process starts with a generation of 2D underlying matrix (all 1's) of size 2392×1417 for all antennas except ($m = 4$, $n = 4$) and ($m = 5$, $n = 4$). For these two antennas 3780×6378 matrix is used. The higher number is to ensure that the sides of antenna are at least one pixel wide. The elements corresponding to the fractal geometry are then made zero. This is the digitization of the fractal antennas in logical array. Then gliding box algorithm is used to calculate the lacunarity of each geometry, including Von Koch. To obviate the effect of box size, the box size weighted average is calculated as suggested in [25, 26] and plotted in Fig. 6. Lacunarity gives information about the non-uniformity in the image. Higher the average lacunarity Λ_{avg}, more is the non-uniformity. This leads to higher resonant frequency as explained by authors in [25]. From Fig. 6, $m = 2$ and $m = 3$ family has lower Λ_{avg} than Koch curve. Lacunarity dimension of $m = 4$ family matches quite closely with the Koch curve, while that of $m = 5$ exceeds it. This behaviour also matches directly with the resonance characteristics explored above. A close observation of Fig. 6 shows that the even ($m = 2$ and $m = 4$) and the odd family ($m = 3$ and $m = 5$) family of fractals have different curve slope. The slope of odd family curve is almost linear while it decreases slowly for the even family. This can explained by looking into the geometry of $m = 2$ and $m = 3$ family as shown in Fig. 1. Comparing iteration 2 of $m = 2$ and $m = 3$, it can be seen that the geometry maintains better uniformity for $m = 3$, whereas L-type sections are created for $m = 2$. This non-uniformity in even family leads to increase in the lacunarity dimension which is cumulatively added with the increasing iteration number. Hence, the slope of Λ_{avg} decreases for even values of m, but stays same for the odd values.

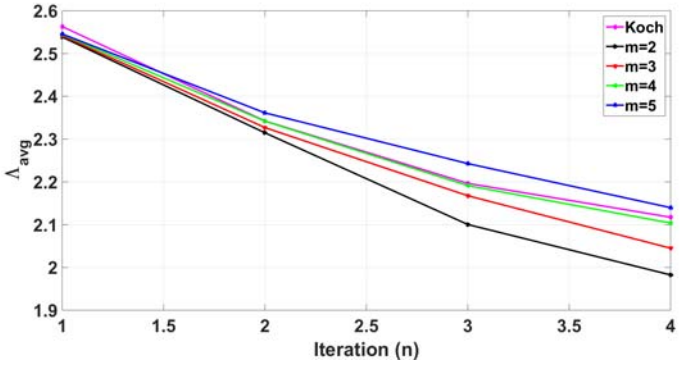

Figure 6. Average lacunarity as a function of iteration number.

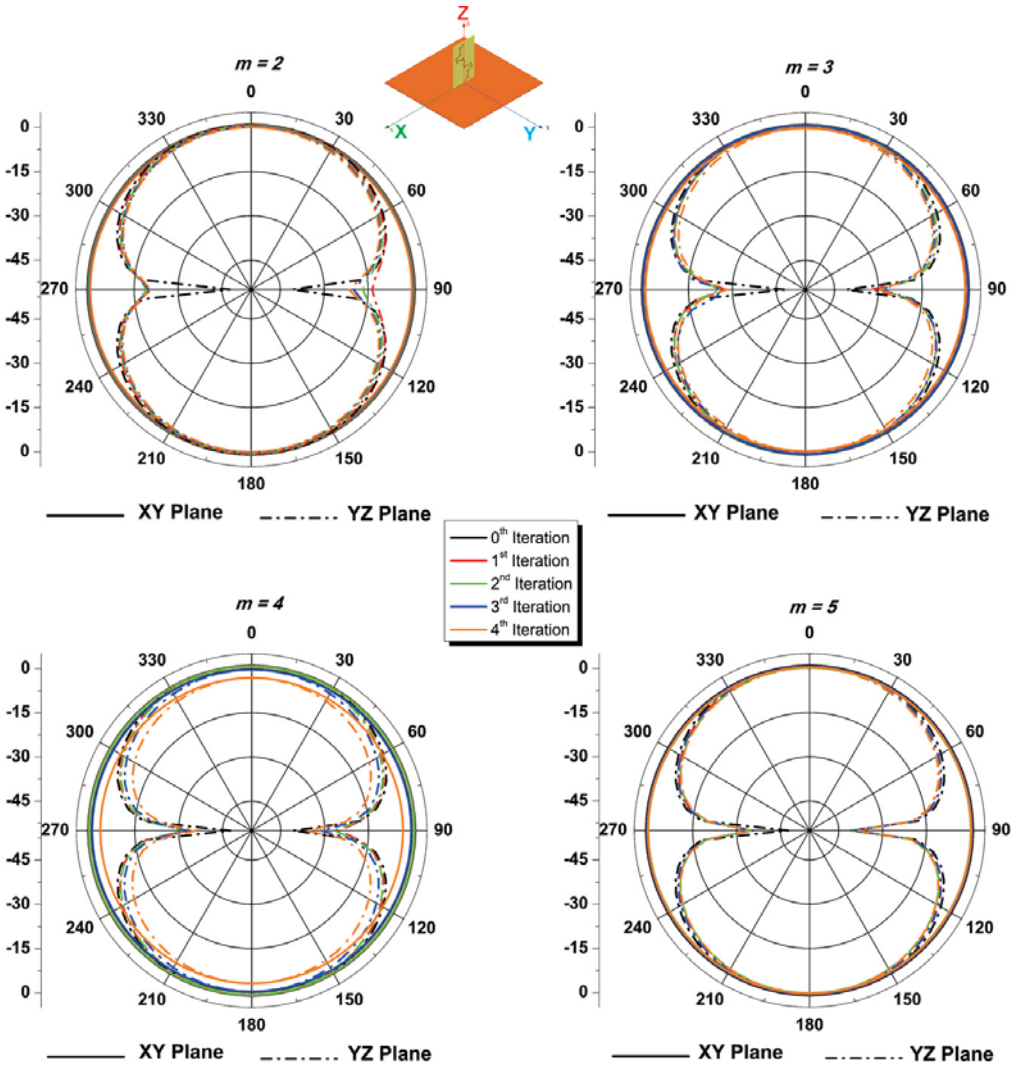

Figure 7. Radiation patterns of 4 families ($m = 2$ to $m = 5$) of proposed fractal curves.

The radiation patterns for different values of m, at their respective resonant frequencies, are plotted in Fig. 7. It can be clearly seen that there is virtually no degradation of radiation pattern as the fractal iteration progresses. It is omnidirectional in the XY plane and bidirectional in the YZ plane. The symmetry of the fractals around the initial generator (straight line monopole) ensures that the radiation pattern is not distorted. This is also a remarkable property of this fractal. Along with providing an extra degree of freedom in terms of form factor and resonant frequency, the proposed construct also maintain its symmetry which leads to such good and clean radiation patterns. From Fig. 7, it can be seen that the gain slightly decreases with increasing iteration number. This may be because of the decreasing radiation efficiency with the increasing iteration. The nulls along z direction are not so sharp for lower values of m and n. The nulls start to become prominent as either iteration number n or seed value m increases. This may be because as the seed value m increases, the width of antenna decreases and it tends to be more like a linear monopole. Also, as the iteration number n increases, the resonant frequency of antenna decreases. In other words, the antenna becomes electrically small and the radiation pattern approaches to that of the linear monopole. Thus, from radiation point of view, if deep nulls are required along the direction of antenna, higher values of m and n are suitable at the cost of increased complexity, whereas smaller values of m and n give more omnidirectional coverage, although radiation is still about 17 dB less than that at the broadside.

5. CONCLUSION

A new family of fractal curves is proposed. The method of generating this curve and the equations characterizing the family are also presented. About 16 antennas based on the proposed fractal geometry are designed and compared against the straight monopole, and the amount of possible miniaturization is quantified by curve fitting the experimental data. The lacunarity dimension analysis is also consistent with the resonance phenomenon observed. It also captures the subtle nuances of the even and odd family of the fractal curves. The symmetry of the proposed fractals ensures that there is no distortion of radiation pattern with increasing iterations. Since the proposed construct depends upon two integer values m and n, the designer has the freedom of optimizing the microwave circuits with different frequency responses and different form factors. The proposed family of fractals can be used as resonators for miniaturizing the microwave components such as Antennas, Microwave filters, Frequency Selective Surfaces (FSS) and Electromagnetic Band Gap structures.

REFERENCES

1. Baliarda, C. P., J. Romeu, and A. Cardama, "The Koch monopole: A small fractal antenna," *IEEE Transactions on Antennas and Propagation*, Vol. 48, No. 11, 1773–1781, 2000.
2. Werner, D. H. and S. Ganguly, "An overview of fractal antenna engineering research," *IEEE Antennas and Propagation Magazine*, Vol. 45, No. 1, 38–57, 2003.
3. Best, S. R., "A discussion on the significance of geometry in determining the resonant behavior of fractal and other non-Euclidean wire antennas," *IEEE Antennas and Propagation Magazine*, Vol. 45, No. 3, 9–28, 2003.
4. Chen, W. and G. Wang, "Effective design of novel compact fractal-shaped microstrip coupled-line bandpass filters for suppression of the second harmonic," *IEEE Microwave and Wireless Components Letters*, Vol. 19, No. 2, 74–76, 2009.
5. Sharma, S., R. Kumar, R. V. S. Ram Krishna, and R. Khokle, "Design of defected ground bandpass filters using stepped impedance resonators," *Progress In Electromagnetics Research B*, Vol. 54, 203–225, 2013.
6. Volakis, J. L., C. Chen, and K. Fujimoto, *Small Antennas: Miniaturization Techniques and Applications*, McGraw Hill Publications, 2010.
7. Gianvittorio, J. P. and Y. Rahmat-Samii, "Fractal antennas: A novel antenna miniaturization technique, and applications," *IEEE Antennas and Propagation Magazine*, Vol. 44, No. 1, 20–36, 2002.
8. Werner, D. H., R. L. Haupt, and P. L. Werner, "Fractal antenna engineering: The theory and design of fractal antenna arrays," *IEEE Antennas and Propagation Magazine*, Vol. 41, No. 5, 37–59, 1999.
9. Mahatthanajatuphat, C., S. Saleekaw, P. Akkaraekthalin, and M. Krairiksh, "A rhombic patch monopole antenna with modified Minkowski fractal geometry for UMTS, WLAN, and mobile WiMAX application," *Progress In Electromagnetics Research*, Vol. 89, 57–74, 2009.
10. Khan, O. M., Z. U. Islam, I. Rashid, F. A. Bhatti, and Q. U. Islam, "Novel miniaturized Koch pentagonal fractal antenna for multiband wireless applications," *Progress In Electromagnetics Research*, Vol. 141, 693–710, 2013.
11. Mahatthanajatuphat, C., P. Akkaraekthalin, S. Saleekaw, and M. Krairiksh, "A bidirectional multiband antenna with modified fractal slot fed by CPW," *Progress In Electromagnetics Research*, Vol. 95, 59–72, 2009.
12. Li, D. and J.-F. Mao, "Multiband multimode arched bow-shaped fractal helix antenna," *Progress In Electromagnetics Research*, Vol. 141, 47–78, 2013.
13. Li, D. and J.-F. Mao, "Sierpinskized Koch-like sided multifractal dipole antenna," *Progress In Electromagnetics Research*, Vol. 130, 207–224, 2012.
14. Farswan, A., A. K. Gautam, B. K. Kanaujia, and K. Rambabu, "Design of Koch fractal circularly polarized antenna for handheld UHF RFID reader applications," *IEEE Transactions on Antennas and Propagation*, Vol. 64, No. 2, 771–775, 2016.

15. Dhar, S., K. Patra, R. Ghatak, B. Gupta, and D. R. Poddar, "A dielectric resonator-loaded Minkowski fractal-shaped slot loop heptaband antenna," *IEEE Transactions on Antennas and Propagation*, Vol. 63, No. 4, 1521–1529, 2015.
16. Jalil, M. E. B., M. K. Abd Rahim, N. A. Samsuri, N. A. Murad, H. A. Majid, K. Kamardin, and M. Azfar Abdullah, "Fractal Koch multiband textile antenna performance with bending, wet conditions and on human body," *Progress In Electromagnetics Research*, Vol. 140, 633–652, 2013.
17. Azaro, R., F. D. Natale, M. Donelli, E. Zeni, and A. Massa, "Synthesis of a prefractal dual-band monopolar antenna for GPS applications," *IEEE Antennas and Wireless Propagation Letters*, Vol. 5, No. 1, 361–364, 2006.
18. Azaro, R., G. Boato, M. Donelli, A. Massa, and E. Zeni, "Design of a prefractal monopolar antenna for 3.4–3.6 GHz Wi-Max band portable devices," *IEEE Antennas and Wireless Propagation Letters*, Vol. 5, No. 1, 116–119, 2006.
19. Ghatak, R., D. R. Poddar, and R. K. Mishra, "Design of Sierpinski gasket fractal microstrip antenna using real coded genetic algorithm," *IET Microwaves, Antennas and Propagation*, Vol. 3, No. 7, 1133–1140, 2009.
20. Donelli, M. and P. Febvre, "Design of a superconducting antenna integrated with a diplexer for radio-astronomy applications," *Journal of Telecommunications and Information Technology*, Vol. 3, 113–118, 2014.
21. Ma, Y., H.-W. Zhang, Y. Li, Y. Wang, and W. Lai, "Terahertz sensing application by using fractal geometries of split-ring resonators," *Progress In Electromagnetics Research*, Vol. 138, 407–419, 2013.
22. Miyamoto, Y., H. Kanaoka, and H. Kirihara, "Terahertz wave localization at a three-dimensional ceramic fractal cavity in photonic crystals," *Journal of Applied Physics*, Vol. 103, 103106, 2008.
23. Sangawa, U., "The origin of electromagnetic resonance in three-dimensional photonic fractals," *Progress In Electromagnetics Research*, Vol. 94, 153–173, 2009.
24. De la Mata Luque, T. M., N. R. K. Devarapalli, and C. G. Christodoulou, "Investigation of bandwidth enhancement in volumetric left-handed metamaterials using fractals," *Progress In Electromagnetics Research*, Vol. 131, 185–194, 2012.
25. Sengupta, K. and K. J. Vinoy, "A new measure of lacunarity for generalized fractals and its impact in the electromagnetic behaviour of Koch dipole antennas," *Fractals*, Vol. 14, No. 4, 271–282, 2006.
26. Comisso, M., "On the use of dimension and lacunarity for comparing the resonant behavior of convoluted wire antennas," *Progress In Electromagnetics Research*, Vol. 96, 361–376, 2009.